

## Effect of Component Thickness and Anode Composition on the Residual Stress of Micro-Tubular Solid Oxide Fuel Cell

Shichuan Su, Wenxuan Zhang\*, Jie Wu, and Congcong Zhou

School of Energy and Power Engineering, Jiangsu University of Science and Technology, 212003, Zhenjiang, Jiangsu, China

\*E-mail: [ZhangWenxuan639@126.com](mailto:ZhangWenxuan639@126.com)

Received: 10 July 2017 / Accepted: 11 August 2017 / Published: 12 September 2017

---

The residual stress of micro-tubular solid oxide fuel cell (MT-SOFC) was investigated by a two-dimensional axisymmetric model. The mechanical stability of anode, electrolyte and cathode was evaluated with the consideration of Ni volume fraction and layer thickness. The results reveal that the high Ni volume fraction in anode is detrimental to the mechanical stability of MT-SOFC: when the Ni volume fraction is more than 50% in solid, it will be hard to keep the integrity of every cell layer within a reasonable thickness range. In order to facilitate the cell design, a minimum anode thickness formula for safe and durable operation was proposed as a function of the Ni volume fraction, electrolyte thickness and cathode thickness. This work simultaneously considered both the Ni volume fraction and layer thickness, which provided a more realistic estimation about MT-SOFC mechanical stability.

---

**Keywords:** Micro-tubular solid oxide fuel cell (MT-SOFC); anode composition; component thickness; residual stress; failure probability.

### 1. INTRODUCTION

Solid oxide fuel cell (SOFC) is electrochemical reaction device that transforms electricity directly from chemical energy. Thus, SOFC is more efficient than combustion-based power generation technologies [1-3]. Meanwhile, SOFC can be operated reversely as solid oxide electrolyzer cells (SOEC) to store the renewable energy in hydrogen or syngas [4-6]. As a result, SOFC will be a promising candidate to cope with the urgent energy shortage and the renewable energy storage faced by modern society [7, 8].

The most mature SOFC designs are planar SOFC (P-SOFC) and tubular SOFC (T-SOFC) [9, 10], each of them has pros and cons: P-SOFC has the advantage of high power density and facility of

massive fabrication, but it suffers thermal instability and gas sealing problem. On the other hand, T-SOFC offers high mechanical strength and gas sealing convenience, although it has lower power density and higher costs [11]. Demonstrated by Singhal and Kendall in early 1990s [12], micro-tubular SOFC (MT-SOFC) is a variant of T-SOFC which shrunk to sub-millimeter scale. Compared to T-SOFC that is typically on the scale of centimeters, the MT-SOFC not only further enhanced the aforementioned advantages of T-SOFC but also brings other benefits, such as high power density, high mass/heat transfer efficiency and rapid start-up/shut-down capability [13-15]. All those characters make MT-SOFC applicable for portable and mobile devices [16].

To achieve the commercialization of MT-SOFC, the manufacture cost and durability are main concerns [17]. Due to the brittle nature of the ceramic, structural failure occurs during fabrication and operation, which directly results in the high cost and short lifespan. In order to understand the mechanical behavior and improve the structure stability of MT-SOFC, a lot of works have been done. For the experiment part, Sammes et al. [18] constructed a custom burst-test instrument to obtain the average strength values of different types of small ceramic tubes. Sin et al. [19] also adopted internal burst-test and c-ring test to get the mechanical properties of MT-SOFC. Although lack of agreements between those two methods, it still seemed apparent that increasing the pore former and wall thickness or decreasing the sintering temperature will induce less hoop stress. Maniet al. [20] compared the mechanical behavior of co-extruded multi-layer half-cells with the conventionally extruded single layer samples, in which the former showed a higher reliability. On the other hand, the cost-effective and time-efficient mathematical model has provided more valuable information, especially on the stress distribution and evolution, which are hard to get experimentally. Cui et al. [21, 22] built a 2D axisymmetric model to study the thermal-fluid behavior, electrochemical reaction and thermal stress of the MT-SOFC. The principal stress shows that the anode suffers tensile stress while the electrolyte and cathode are under compressive stress. They also performed the Weibull failure analyses at different loads. It is concluded that the stress in the membrane electrode assembly (MEA) is mainly due to the residual stress induced by the mismatch between thermal expansion coefficients (TEC) and the anode is the determining factor to keep the MEA safe. In order to improve reliability, matching the deformation by adjusting anode TEC is a possible way. However, they did not investigate the residual stress at ambient temperature and their model did not consider the effects of electrode compositions on thermal stress of the MT-SOFC. Lin et al. [23, 24] filled this research gap in their papers. Their model included the effects of Ni and La(Sr)MnO<sub>3</sub> (LSM) compositions on the electrochemical and mechanical performance. It turns out that a high Ni volume fraction in anode is unfavorable for mechanical stability. However, the LSM in cathode is inconsequential for mechanical behavior and should be optimized according to the requirement of electrochemical performance. Serincan et al. [25] studied the stress in fabrication and operation. Their model included the impact of test fixture and the electrolyte gadolinia-doped ceria (GDC) reduction. The effects of sealant and alumina tube on the stress distribution are found to be significant. They also distinguished the residual stress and the stress induced by temperature gradient and found that the effect of the temperature distribution is minimal for mid-range current densities.

Despite those fruitful works, none of them considered the MEA components (including anode, electrolyte and cathode) thickness. However, the component thickness can be a key parameter for the

stress condition of MT-SOFC, which has been proved in our previous paper [26]. In that work, the influence of component thickness on the residual stress has been systematically revealed without the consideration of composition. However, the electrodes are porous composite material and the effect of composition and thickness should be considered simultaneously. On the one hand, the compositions have significant influence on the strain and stress [27]. On the other hand, the thickness is also the decisive factor for the stress conditions. Therefore, thickness should match with composition to keep the integrity of every component. In order to provide a comprehensive understanding of mechanical behaviors of MT-SOFC, this paper aims to systematically study the effects of composition and thickness on residual stress. Such a detailed study will provide better understanding and prediction about MT-SOFC mechanical behaviors.

## 2. MODEL DESCRIPTION

This work focus on the residual stress in MT-SOFC due to the TEC mismatch between the MEA components. The anode supported MT-SOFC is considered here, as shown in Fig. 1(a). The YSZ electrolyte is sandwiched between the Ni-YSZ anode and LSM-YSZ cathode, as in Fig. 1(b). As long as the temperature deviated from the stress free temperature, different shrinkages between MEA layers will induce residual stress, but room temperature is the most critical condition that an MT-SOFC may experience because the temperature difference from the stress free temperature is the maximum. So the following study will be based on the residual stress at room temperature. Considering the axial symmetry, the 3D MT-SOFC model can be simplified into a 2D axisymmetric model as shown in Fig. 1(b).

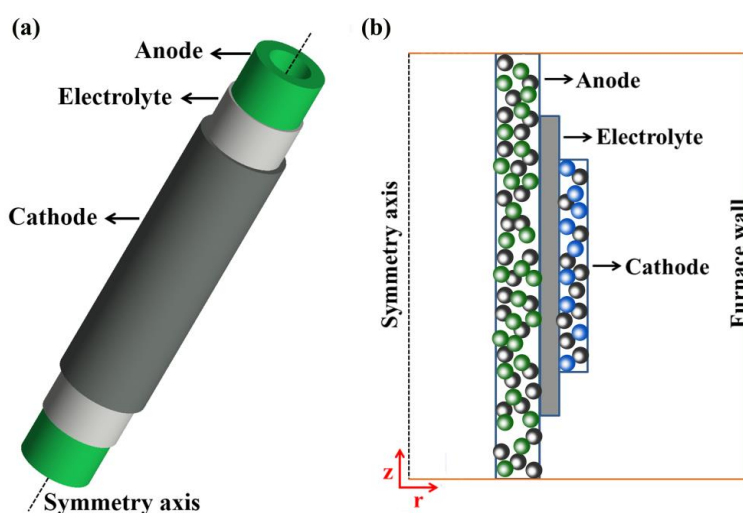


**Figure 1.** Schematic of the (a) 3D MT-SOFC and (b) 2D axisymmetric MT-SOFC model

Since this is a further study based our previous work in paper [26], the related geometry parameters, material properties, constitutive equations and model verification are the same, which will not be repeated here.

### 3. RESULT AND DISCUSSION

#### 3.1 Material properties

The electrode composition has a significant influence on its mechanical properties. As concluded in paper [22], anode is the decisive factor for MEA mechanical stability, so we will focus on manipulating the Ni volume fraction of anode in order to study its impact on MEA stress. However, the immediate effect of Ni composition is on anode mechanical properties, as shown in Fig. 2. The relationships between Young's modulus, Poisson ratio and the anode Ni volume fraction at room temperature are described in Fig. 2a, in which both of them show minor reductions with the increase of Ni composition due to similar Young's modulus and Poisson ratios between Ni and YSZ [28]. However, the TEC of Ni is much larger than YSZ [29, 30], which gives the anode TEC a significant rise with the increase of Ni volume fraction, as shown in Fig. 2b. Since the TEC mismatch between MEA layers is the main cause of residual stress, the Ni volume fraction must have a tremendous effect on the MT-SOFC stress.

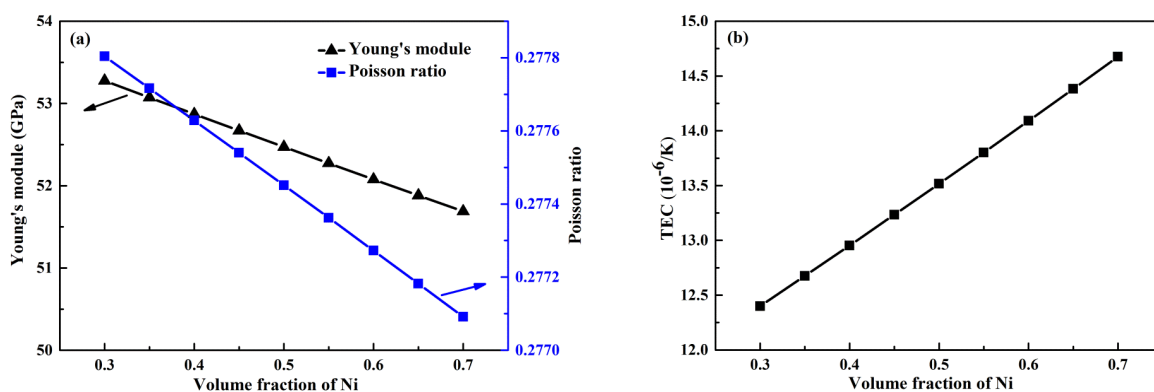


**Figure 2.** The anode mechanical properties as a function of the Ni volume fraction (a) the effective Young's module and Poisson ratio; (b) the effective TEC.

#### 3.2 The residual stress of anode

The influence of the Ni volume fraction on the maximum principal stress of anode is shown in Fig. 3, in which the thickness of electrolyte and cathode are fixed as 20  $\mu\text{m}$  and 60  $\mu\text{m}$  respectively. On the one hand, tensile stress suffered by anode increases with the increase of Ni volume fraction primarily due to the larger anode TEC resulting from high Ni composition. This is because the anode must shrink more while cooling down but the electrolyte and cathode cannot keep up with it, leading to larger tensile stress. On the other hand, anode tensile stress decreases with thicker anode. According to the force equilibrium, the integral of anode tensile stress over its volume is equal to the integral of electrolyte and cathode compression stress with an opposite sign. Due to the fixed electrolyte and cathode dimensions, tensile stress of anode can be reduced by thickening anode component.

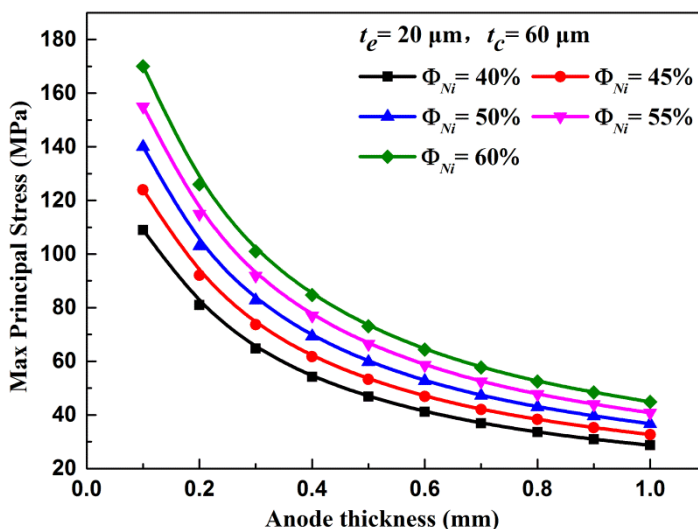


Figure 3. The effects of Ni volume fraction on the max principal stress of anode

### 3.3 Failure probability analysis of anode

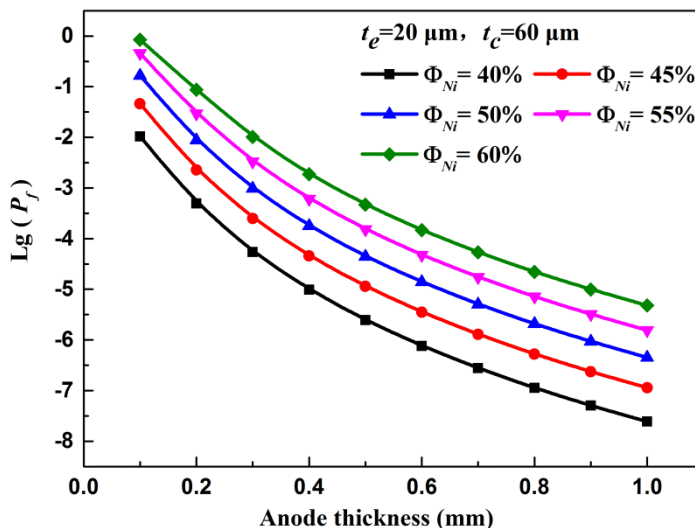


Figure 4. The effects of Ni volume fraction on the anode failure probability

Since the anode is under tension, its failure probability can be assessed by Weibull approach [31, 32]. The fatigue failure probability standard of SOFC is usually set as 1E-6 to ensure the mechanical stability of practical application [33]. Fig. 4 shows the anode failure probability at different Ni compositions and anode thicknesses. The high Ni composition and the thin anode will result in high failure risk, which is in accordance with the behavior of max principle stress in Fig. 3. In order to meet the failure criterion of 1E-6, the minimum thicknesses required for anode are 0.566 mm, 0.699 mm, 0.877 mm when Ni volume fractions are 40%, 45%, 50%, respectively. However, for higher Ni

compositions like 55% and 60%, it is impossible to guarantee the anode safety in the range of 0.1 mm-1 mm, which clearly demonstrates the importance to simultaneously consider the impacts of composition and thickness.

Based on the above stress and failure probability analyses of anode in Section 3.2 and Section 3.3, the Ni volume fraction should be kept under 50% in order to ensure the anode integrity. Meanwhile, the electrochemical performance can still be greatly improved under this condition [34].

### 3.4 The minimum anode thickness with various Ni volume fractions

The previous results strongly indicate that with the given Ni volume fraction and the electrolyte and cathode thicknesses, the anode must ensure a minimum thickness  $t_a$  in order to keep the failure probability below  $1E-6$ , explicitly drawing the relationship between those parameters will be helpful for cell design. Shown in Fig. 5 is the relationship among the thicknesses of anode/electrolyte/cathode under 40 and 60% Ni volume fraction. The plot shows that the minimum anode thickness increases with increasing cathode and electrolyte thickness, because of the same force equilibrium reason mentioned before. The phenomenon is consistent with previous studies [26]. However, the minimum anode thickness is more sensitive to electrolyte thickness than that of cathode, which is in accord with earlier research [37], the electrolyte thickness had pronounced effect on the stress while the influence of cathode thickness is marginal. Taking the case with 40% Ni volume fraction, 10  $\mu\text{m}$  cathode and 10  $\mu\text{m}$  electrolyte as an example, when electrolyte thickness is increased to 20  $\mu\text{m}$ , the minimum anode thickness is increased 0.378 mm, but even when cathode thickness is increased to 60  $\mu\text{m}$ , minimum anode thickness is only increased 0.197 mm, about half of increment caused by electrolyte. Besides, it is apparent that the minimum requirement for anode thickness improved with the increase of Ni composition. Because higher Ni volume fraction enlarges the TEC mismatch between anode and other MEA layers [23], which will induce larger residual stress, the anode volume must be increased to balance it in case of failure.

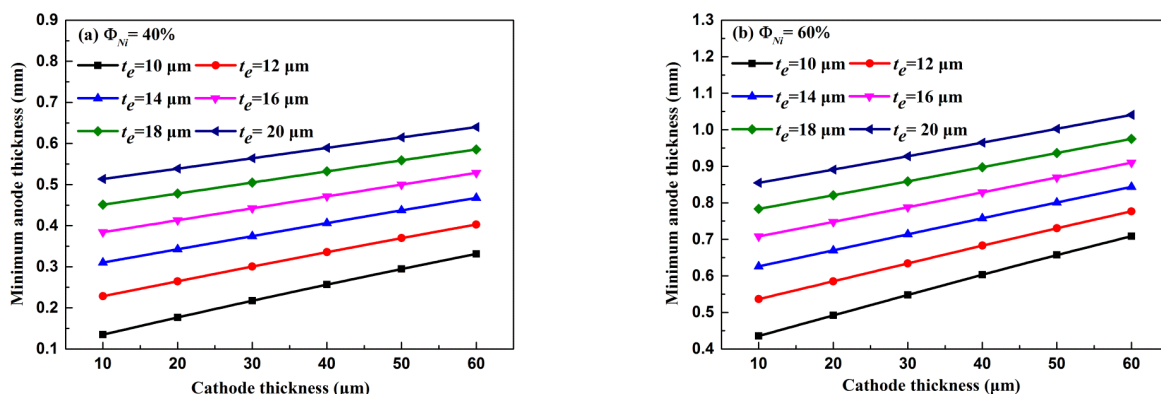


**Figure 5.** The relationship among the thicknesses of anode/electrolyte/cathode under: (a) 40% Ni volume fraction; (b) 60% Ni volume fraction.

For the given Ni volume fraction and electrolyte thickness, the minimum anode thickness is related to the cathode thickness via following correlation:

$$t_{\text{min-anode}} = A + B \times t_{\text{cathode}} \tag{1}$$

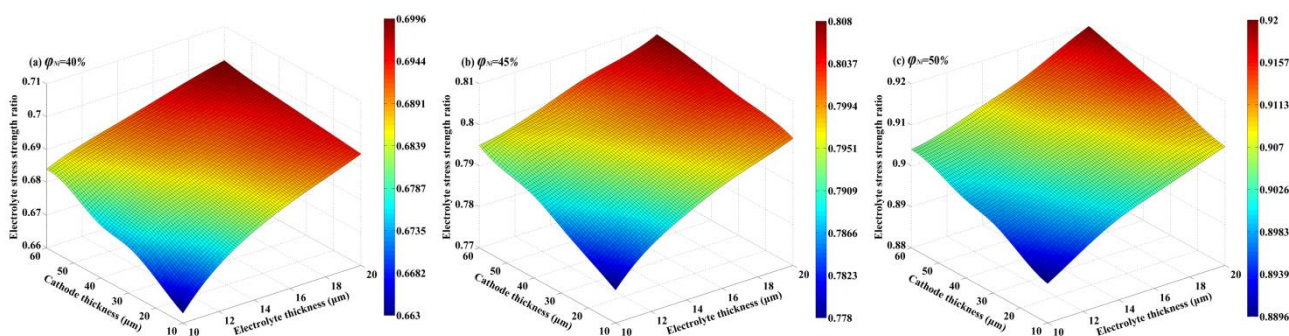
where  $A$  is intercept and  $B$  is slop. Besides, the unit of the  $t_{\text{cathode}}$  and  $A$  are [ $\mu\text{m}$ ], and the unit of  $B$  is 1. The values of  $A$  and  $B$  corresponding to different Ni volume fraction and electrolyte thickness are shown in Table 1. In this fashion, the Ni composition and the component thickness are fully coupled, so the revealed relationship is comprehensive and reliable, which brings considerable convenience to the design of MT-SOFC.

**Table 1.** The value of intercept  $A$  and slop  $B$

Electrolyte thickness ( $\mu\text{m}$ )		10	12	14	16	18	20
$\varphi_{\text{Ni}}=40\%$	$A$	165.2	218.7	269.9	319.8	369.2	419.1
	$B$	2.3	2.3	2.3	2.3	2.3	2.4
$\varphi_{\text{Ni}}=45\%$	$A$	209.3	268.2	325.0	381.2	437.8	495.7
	$B$	2.8	2.8	2.9	2.9	3.1	3.3
$\varphi_{\text{Ni}}=50\%$	$A$	251.0	315.0	375.7	440.1	504.1	566.9
	$B$	3.4	3.4	3.6	3.8	4.2	5.0
$\varphi_{\text{Ni}}=55\%$	$A$	289.5	368.3	426.4	491.6	549.7	668.8
	$B$	4.0	3.8	4.5	5.1	6.7	6.5
$\varphi_{\text{Ni}}=60\%$	$A$	324.4	397.1	465.1	540.8	644.9	787.8
	$B$	4.8	5.2	6.1	7.4	8.7	8.7

### 3.5. The effects of Ni volume fraction on the electrolyte and cathode

After the formulation of minimum anode thickness, we will take it as a precondition to further verify the stability of electrolyte and cathode. Both electrolyte and cathode endure compressive stress due to smaller TECs comparing to anode. For ceramic material, when the compressive stress exceeds the compressive strength, it will cause fracture.



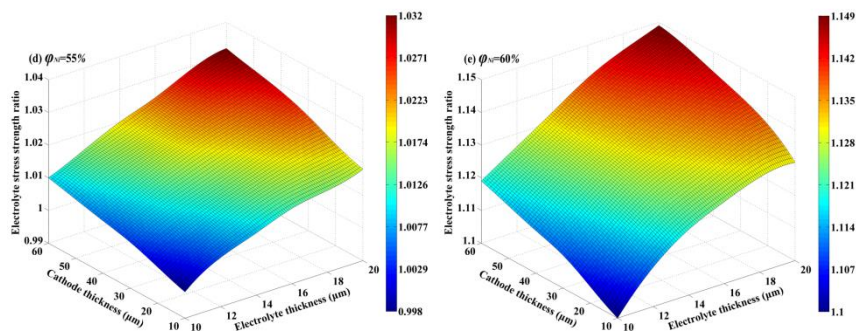


**Figure 6.** The effects of Ni volume fraction (a)40%; (b)45%; (c)50%; (d)55% and (e)60% on the electrolyte risk ratio

Since Weibull method can only be applied to tensile stress, the ratio of the maximum compressive stress to the compressive strength will be adopted as the indicator for risk evaluation under compressive stress (hereinafter cited as risk ratio). For the electrolyte and cathode, the compressive strengths are 1 GPa [35] and 100 MPa [36], respectively.

Fig. 6 presents the electrolyte risk ratio as a function of cathode thickness, electrolyte thickness and Ni volume fraction.

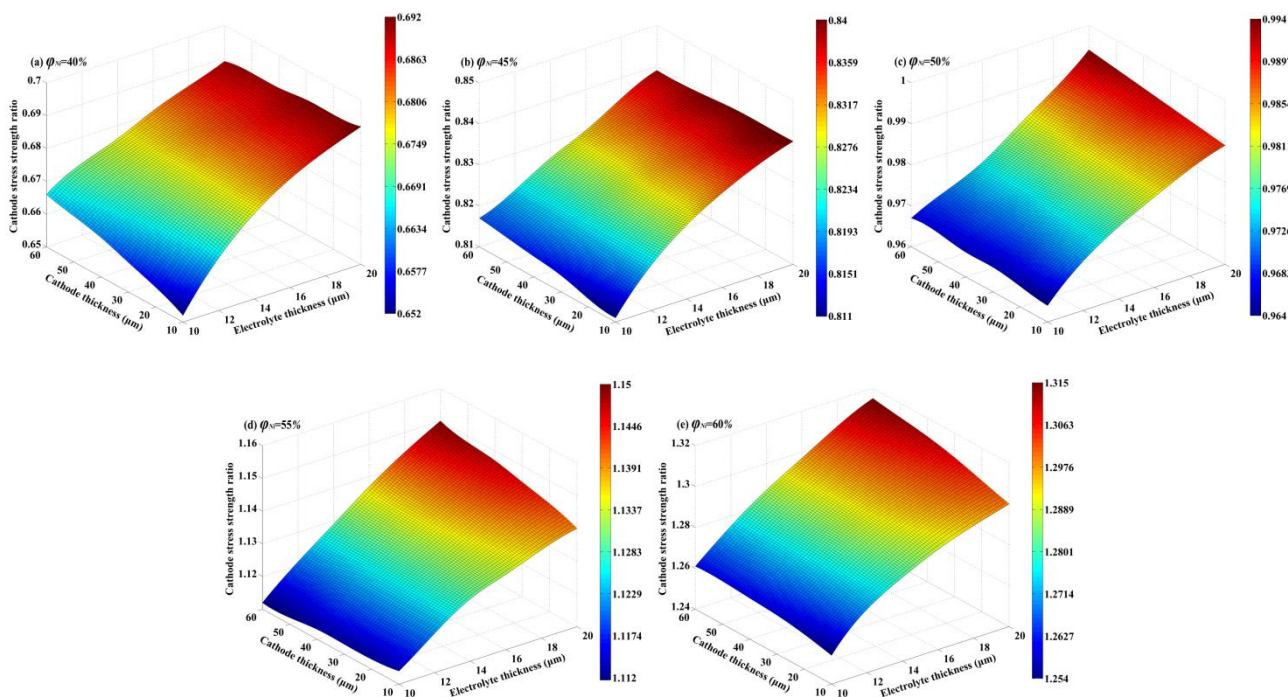


**Figure 7.** The effects of Ni volume fraction (a)40%; (b)45%; (c)50%; (d)55% and (e)60% on the cathode risk ratio

For the anode, minimum thickness obtained by Eq. 1 is employed here. At first, with the volume fraction of Ni increased from 40% to 60%, the lower bound of the risk ratio increased significantly, from 0.663 to 1.1. Particularly, at the high Ni volume fractions of 55% and 60%, the risk



ratio is above 1 in the whole scope, which means the electrolyte cannot survive in those configurations. The reason is obvious: the anode needs to shrink more while cooling down due to the larger TEC induced by a high Ni composition, therefore, the compression suffered by electrolyte and cathode dramatically increased. In previous paper [23,24], the authors showed that the electrolyte maximum stress wouldn't surpass the compressive strength (the risk ratio wouldn't surpass 1) when the Ni volume fractions is 0.6, which is exactly similar to this study. The slight difference may be caused by the different thickness. And second, when the Ni volume fraction is fixed, the risk ratio increases with the increase of electrolyte thickness or cathode thickness. Because with the thickening of cathode and electrolyte, the minimum anode thickness is also increasing (Fig. 5), which will cause larger compression stress in electrolyte, so the risk ratio goes up.

The cathode risk ratio is displayed in Fig. 7, which is similar to the electrolyte risk ratio. The high Ni volume fraction is unfavorable for cathode safety. Meanwhile, the electrolyte thickness has a much more significant influence on the risk ratio than cathode thickness. The reason still lies in Fig. 5, because the minimum anode thickness is more sensitive to electrolyte thickness, so with the same thickness additions, the electrolyte increment will result in a thicker anode, which in return introduces larger compression.

Combining the results of Section 3.3 and 3.5, we can conclude that the anode Ni composition must be kept below 50% in order to ensure safety of the whole MEA.

#### 4. CONCLUSIONS

Based on the developed 2D axisymmetric stress model, the residual stress of MT-SOFC was investigated by simultaneously considering the effects of Ni volume fraction and MEA component thickness. It is found that high Ni composition will give rise to the high anode failure probability, but this can be counterbalanced by increasing anode thickness. Then, the minimum anode thickness was formulated as the function of Ni volume fraction, electrolyte thickness and cathode thickness, which will bring considerable convenience for cell design. Finally, a high Ni fraction was proved to be unfavorable for electrolyte and cathode stability and it is impossible to keep the stability of electrolyte and cathode when Ni composition is above 50%. Considering the safety of the whole MEA, the maximum anode Ni volume fraction should be 50%.

#### ACKNOWLEDGEMENTS

We gratefully acknowledge the financial support of the National Science Foundation of China (21406095), and the Jiangsu Province Colleges and Universities Natural Science Projects (13KJB480003).

#### References

1. S. Molla, T.T, Kwok. K and Frandsen. HL, *Int. J. Hydrogen Energy*, 41 (2016) 6433.
2. S. Su, X. Gao, Q. Zhang, W. Kong and D. Chen, *Int. J. Electrochem. Sci.*, 10 (2015) 2487.

3. B. Xiao, X. Jiang and Q. Jiang, *Chem. Phys.*, 18 (2016) 30174.
4. Pan. Z, Liu. Q, Zhang. L, Zhou. J, Zhang. C and Chan. SH, *Appl. Energy*, 191 (2017) 559.
5. Kim. SJ, Kim. KJ and Choi. GM, *Int. J. Hydrogen Energy*, 40 (2015) 9032.
6. Kushi. T, *Int. J. Hydrogen Energy*, 42 (2017) 9396.
7. D. Chen, Q. Zhang, L. Lu, V. Periasamy, M.O. Tade and Z. Shao, *J. Power Sources*, 303 (2016) 305.
8. W. Kong, Q. Zhang, X. Gao, J. Zhang, D. Chen and S. Su, *Int. J. Electrochem. Sci.*, 10 (2015) 2487.
9. Timurkutluk. B, Timurkutluk. C, Mat. MD and Kaplan. Y, *Renew. Sustain. Energy Rev.*, 56 (2016) 1101.
10. Z. Yu, S. Liu, F. Zheng, W. Kong and Y. Ding, *Int. J. Electrochem. Sci.*, 11 (2016) 10210.
11. Jamil. SM, Othman. MHD, Rahman. MA, Jaafar. J, Ismail. AF and Li. K, *J. Eur. Ceram. Soc.*, 35 (2015) 1.
12. Kendall. SCSK, High temperature Solid Oxide Fuel Cells---Fundamentals, Design and Applications, *Elsevier Advanced Technology*, (2003) Kidlington, UK.
13. Meng. X, Gong. X, Yang. N, Tan. X, Yin. Y and Ma. Z-F, *J. Power Sources*, 237 (2013) 277.
14. Ahmad. SH, Jamil. SM, Othman. MHD, Rahman. MA, Jaafar. J and Ismail. AF, *Int. J. Hydrogen Energy*, 42 (2017) 9116.
15. Kendall. K and Meadowcroft. A, *Int. J. Hydrogen Energy*, 38 (2013) 1725.
16. Dela. Torre. R and Sglavo. VM, *Int. J. Appl. Ceram. Tec.*, 9 (2012) 1058.
17. Zouhri. K and Lee. S-Y, *Energy Convers. Manage.*, 121 (2016) 1.
18. N. M and SAMMES. YD, *J. Mater. Sci.*, 38 (2003) 4811.
19. Sin. Y-W, Galloway. K, Roy. B, Sammes. NM, Song. J-H and Suzuki. T, *Int. J. Hydrogen Energy*, 36 (2011) 1882.
20. Mani. B and Paydar. MH, *Ceram. Int.*, 42 (2016) 4194.
21. Cui. D and Cheng. M, *AIChE. J.*, 55 (2009) 771.
22. Cui. D and Cheng. M, *J. Power Sources*, 192 (2009) 400.
23. Li. J and Lin. Z, *Int. J. Hydrogen Energy*, 37 (2012) 12925.
24. Li. J, Kong. W and Lin. Z, *J. Power Sources*, 232 (2013) 106.
25. Serincan. MF, Pasaogullari. U and Sammes. NM, *J. Power Sources*, 195 (2010) 4905.
26. W. Kong, W. Zhang, S. Zhang, Q. Zhang and S. Su, *Int. J. Hydrogen Energy*, 41 (2016) 16173.
27. Chiang. L-K, Liu. H-C, Shiu. Y-H, Lee. C-H and Lee. R-Y, *J. Power Sources*, 195 (2010) 1895.
28. Mounir. H, Belaiche. M, El. Marjani. A and El Gharad A, *Energy*, 66 (2014) 378.
29. Masashi. Mori. TY and Hibiki. Itoh, *Int. J. Electrochem. Sci.*, 145 (1998) 1374.
30. Johnson. J and Qu. J, *J. Power Sources*, 181 (2008) 85.
31. Weibull. W, *Proceedings of the Royal Swedish Institute of Engineering Research*, 45 (1939) 1.
32. Greco. F, Frandsen. HL, Nakajo. A, Madsen. MF and Van herle J, *J. Eur. Ceram. Soc.*, 34 (2014) 2695.
33. Nakajo. A, Stiller. C, Härkegård. G and Bolland. O, *J. Power Sources*, 158 (2006) 287.
34. Haslam. JJ, Pham. A-Q, Chung. BW, DiCarlo. JF and Glass. RS, *J. Am. Ceram. Soc.*, 88 (2005) 513.
35. Yakabe. H, Baba. Y, Sakurai. T and Yoshitaka. Y, *J. Power Sources*, 135 (2014) 9.
36. Liu. X, Martin. CL, Bouvard. D, Di. Iorio S, Laurencin. J and Delette. GS, *J. Am. Ceram. Soc.*, 94 (2011) 3500.
37. Zhang. T, Zhu. Q, Huang. W, Xie. Z and Xin. X, *J. Power Sources*, 182 (2008) 540.